Geomorphology 267 (2016) 25–36

Contents lists available at ScienceDirect

Geomorphology

journal homepage: www.elsevier.com/locate/geomorph

Spatial patterns of sediment dynamics within a medium-sized watershed over an extreme storm event

Peng Gao *, Zhirou Zhang

Department of Geography, Syracuse University, NY 13244, USA

ARTICLE INFO

Article history:
Received 28 April 2016
Received in revised form 8 May 2016
Accepted 24 May 2016
Available online 26 May 2016

Keywords:
Sediment transport
Extreme event
Watershed modeling
Sediment connectivity

ABSTRACT

In this study, we quantified spatial patterns of sediment dynamics in a watershed of 311 km^2 over an extreme storm event using watershed modeling and statistical analyses. First, we calibrated a watershed model, Dynamic Watershed Simulation Model (DWSM) by comparing the predicted with calculated hydrograph and sedigraph at the outlet for this event. Then we predicted values of event runoff volume (V), peak flow (Q_{peak}), and two types of event sediment yields for lumped morphological units that contain 42 overland elements and 21 channel segments within the study watershed. Two overland elements and the connected channel segment form a first-order subwatershed, several of which constitute a larger nested subwatershed. Next we examined (i) the relationships between these variables and area (A), precipitation (P), mean slope (S), soil erodibility factor, and percent of crop and pasture lands for all overland elements (i.e., the small spatial scale, SSS), and (ii) those between sediment yield, Q_{peak}, A, P, and event runoff depth (h) for the first-order and nested subwatersheds along two main creeks of the study watershed (i.e., the larger spatial scales, LSS). We found that at the SSS, sediment yield was nonlinearly well related to A and P, but not Q_{peak} and h; whereas at the LSS, linear relationships between sediment yield and Q_{peak} existed, so did the Q_{peak}–A, and Q_{peak}–P relationships. This linearity suggests the increased connectivity from the SSS to LSS, which was caused by ignorance of channel processes within overland elements. It also implies that sediment was transported at capacity during the extreme event. So controlling sediment supply from the most erodible overland elements may not efficiently reduce the downstream sediment load.

1. Introduction

A fundamental difficulty of managing sediment dynamics is predicting sediment loads at different temporal (event, seasonal, annual, or decadal) and spatial (plot, reach, or subwatershed) scales (Owens et al., 2005; Walling and Zhang, 2004; Wilkinson and McElroy, 2007). Sediment initiation (i.e., sediment detachment) in source areas and transport through hillslope and stream channels within a watershed are considerably complex (Collins and Walling, 2004; Gao, 2008; Jones and Preston, 2012; Orwin and Smart, 2004; Smith et al., 2011; Turnbull et al., 2008; Vericat and Batalla, 2006; Yair and Kossovsky, 2002).This complexity inherently results from the nonlinear upscaling nature — that is, sediment load at a smaller scale is not proportional to that at a larger one (Cammeraat, 2002; Moreno-de las Heras et al., 2010; Verbist et al., 2010; Zheng et al., 2011). Studies on changes of annual sediment yields measured at the outlets of watersheds spanning a variety of climatic zones and physiographic conditions (de Vente et al., 2006, 2007; van Dijk and Bruijnzeel, 2005) have divulged that the relationship between annual sediment yield and the watershed size (A) not only is generally nonlinear, but also varies from region to region, indicating the complexity of sediment dynamics spatially and temporally.

Consensus on this complexity has catalyzed continuous efforts on exploring interaction of sediment processes among sources and sinks at multiple spatial and temporal scales within a watershed (Cammeraat, 2004; Estrany et al., 2009; Evrard et al., 2011; Favaro and Lamoureux, 2015; Gomi et al., 2005; Navratil et al., 2010; Salant et al., 2008; Underwood et al., 2015). A typical type of approach resorts to quantifying relative contributions of various sediment sources to the downstream sediment yields using sediment budget analysis on hillslope, along the main stream, or through the entire watershed (Belmont et al., 2011; Collins et al., 2010; Fukuyama et al., 2010; Houben, 2008; Rustomji et al., 2008; Walling, 2005; Warrick et al., 2015; Wilkinson et al., 2009; Wilson et al., 2008). Another type of method is grounded on the concept of sediment connectivity, which in a fluvial system, refers to the physical connection of sediment via channel network and to the potential of a soil particle moving from one zone or location to another (Cavalli et al., 2013; Fryirs, 2013; Hooke, 2003; Wethered et al., 2015).

* Corresponding author.
E-mail address: pegao@maxwell.syr.edu (P. Gao).

http://dx.doi.org/10.1016/j.geomorph.2016.05.025
0169-555X/

In either type of methods, a sufficient amount of data describing all possible sediment sources are required to achieve the goals (Belmont et al., 2011; Kabir et al., 2014; Menounos et al., 2006; Wilkinson et al., 2009). Nonetheless, data at this level of detail may not always be available, in particular during extreme storm events when the flooded area is not even physically accessible. This constraint might be eased by characterizing dominant processes of sediment dynamics at relatively coarse spatial and longer time scales because the intricate and highly variable processes of sediment transport at finer spatial and shorter time scales may be averaged off, such that simpler (i.e., dominant) processes may be captured using relatively simple methods (Brasington and Richards, 2007; Cerdan et al., 2004; Hunter et al., 2007; Murray, 2007; Nicholas, 2010). Recently emerged reduced-complexity models (Chen et al., 2014; Czuba and Foufoula-Georgiou, 2014; Murray, 2007; Nicholas, 2010) apparently support this rationale.

Temporally, instantaneous sediment transport is obviously too complex to be described quantitatively (Brown and Chanson, 2012). Instead, the event scale could be a reasonable time scale at which sediment dynamics should be quantitatively characterized for at least three reasons. First, sediment data at this scale are relatively easy to acquire in practice without missing too much sediment variation within an event. Second, our previous studies indicated that annual sediment yields estimated in terms of event sediment yields are not statistically different from those calculated based on instantaneous sediment transport rates (Gao and Josefson, 2012a, 2012b). Third, many studies have shown that event sediment yields from watersheds of different climatic zones and sizes may be well correlated to hydrological variables such as peak discharge and event runoff depth (Gao et al., 2013b; Hicks, 1994; Hicks et al., 2004; Zheng et al., 2008, 2012) and hence may be used to reveal causality of sediment connectivity over multiple spatial scales.

Spatially, if a watershed is divided into a group of lumped morphologic units, such as overland elements connected by channel segments or the combined subwatersheds (Carpenter and Georgakakos, 2006; Jetten et al., 2003), then the averaged size of these units may be referred to as a coarse scale of the watershed in comparison with the smaller size of grid cells (Francipane et al., 2012; Pelletier, 2012; Taguas et al., 2011) forming the same watershed. Many modeling studies concerning fluvial sediment transport at the coarse scales have focused on spatial and temporal distributions of sediment yields or relating these loads to the relatively stable features of these units such as mean slopes and elevations over monthly, annual, decade, or even longer periods (Forzoni et al., 2013; Medeiros et al., 2010; Mills and Bathurst, 2015; Patil et al., 2012; Syvitski and Milliman, 2007; Zhou and Li, 2015). Very few have explored the processes of sediment transport during storm events for the entire watershed and/or isolated subwatersheds (Bisantino et al., 2015; Zhang et al., 2013). Yet, watershed models have not been used to explore spatial variations of sediment transport and their connections within a watershed during a rainfall event, in particular an extreme event that could cause flooding.

This study filled the gap by modeling processes and analyzing spatial changes of sediment transport over multiple spatial scales within a medium-sized watershed during an extreme storm event that had no in situ sediment measurement available from flooding. The analysis was based on the data predicted using a physically based watershed model, Dynamic Watershed Simulation Model (DWSM). In addition, the model generates a set of lumped units that contain a number of overland elements and the associated channel segments. Two overland elements and one channel segment form a subwatershed (termed here first-order subwatershed) and several such subwatersheds form a larger subwatershed. Therefore, the spatial elements of the divided study watershed are consistent with the fundamental geomorphological unit, watershed, which spatially contains hillslopes and their connected streams (Leopold et al., 1964). This consistency facilitates not only separating hillslope from in-channel processes, but also determining spatially variable sediment transport over nested subwatersheds.

We first used DWSM to predict hydrograph and sedigraph at the watershed outlet and compared them with the calculated counterparts for an extreme event. Next, we predicted using DWSM, event runoff volume (V, m^3), peak discharge (Q_{peak}, m^3/s), and event sediment yields for all divided lumped spatial units. Here the total sediment load transported out of a given lumped unit during the event is referred to as total event sediment yield (TSY_e, t), the sediment load per unit area of a given lumped unit is termed area-specific sediment yield (SSY_e, t/m^2). Using these data we then investigated spatial patterns of sediment transport and their links to the associated hydrological processes across multiple spatial scales including overland elements, first-order, and nested subwatersheds.

2. Materials and methods

2.1. Study area and the selected event

The study watershed is the upper and middle parts of Oneida Creek watershed, one of seven subwatersheds comprising Oneida Lake basin in central New York, USA. It is located southeast of the Oneida Lake basin and has an area of 311 km^2 (Fig. 1). The watershed has elevations varying between 123 and 574 m with slopes becoming progressively steeper (up to 59°) from north to south along the west side of the main stream, Oneida Creek. The stream morphology varies from a bedrock upstream reach with a waterfall to downstream gravel-bed reaches with pools and riffles characterized by a mixture of gravel, sand, and silt. Sconondoa Creek, the main branch on the east side, is comparable in size and converges near the outlet of the study watershed to Oneida Creek. Sediment, primarily derived and transported from hillslopes, consists largely of silt- and clay-sized particles and generally moves in suspension. Although Oneida Creek only contributes 7% of the total water inflow to Oneida Lake, it supplies about 22.3% of the total sediment load to the lake (Makarewicz and Lewis, 2003). The lower reach of Oneida Creek has been listed as a prioritized water body that needs to be further studied (CNYRPDB, 2004). The excessive sediment load in the watershed is largely caused by severe soil erosion at dairy farms and in cultivated lands, which also contribute phosphorus, nitrogen, heavy metals, and pesticides along with suspended sediment to the creek (CNYRPDB, 2004), as well as accelerated surface erosion in urban areas because of site construction and road erosion (Gruszowski et al., 2003). City of Oneida is the largest town located around the outlet of the study watershed.

The selected hydrological event was triggered by a storm that happened on 28 June 2013. The storm only lasted for about 12 h (i.e., from midnight to noon). However, it was spatially concentrated with high intensities, such that it generated a historical flood event with the largest peak discharge (Q_{peak}) since the beginning of gauging in 1950 (the recurrence interval of Q_{peak} was 86 years; Gao and Hartnett, 2016). The downtown and its surrounding area of the City of Oneida located within the watershed were substantially inundated. A large amount of suspended sediment carried by flood flow caused severe damages. Investigating spatial variations of sediment dynamics over this event is valuable in theory because these variations reflect the nature of sediment dynamics under the extreme case among all possible storm events in the area. The outcomes of the investigation are also pragmatically useful because they may provide quantitative explanation on how sediment moved from upland (i.e., the small spatial scale) to the downstream channel (i.e., the large spatial scale) during the extreme event and facilitate the future design of management plans.

2.2. Watershed modeling

2.2.1. Model components

The DWSM characterizes dynamic processes of hillslope surface runoff and subsurface flow, hillslope soil erosion and movement, in-channel flow movement, and sediment entrainment and transport

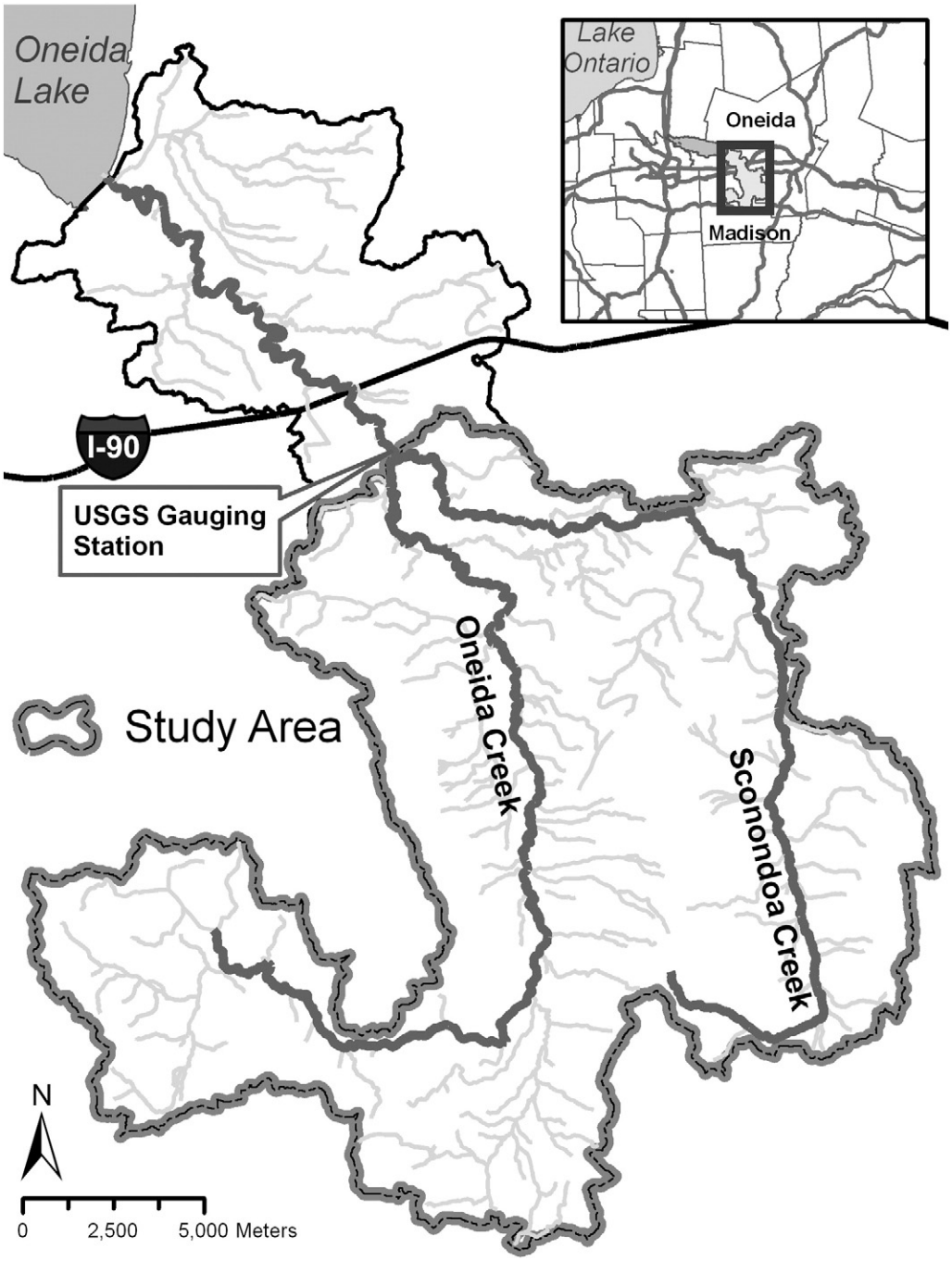

Fig. 1. The study watershed and its two creeks. The watershed outlet is located about 1 km downstream of the USGS gauging station where the two creeks converge.

over a storm event using a set of mathematical equations (Borah et al., 2002, 2004). Surface runoff on hillslopes is determined by (Borah et al., 2007)

$$I_{e,i} = \frac{Q_{r,i} - Q_{r,i-1}}{\Delta t_i} \tag{1}$$

where $I_{e,i}$ (mm/h) is the rainfall excess rate during the time interval Δt_i; and $Q_{r,i}$ (mm) is accumulated direct runoff or rainfall excess at time step i. It is determined using the runoff curve number method (USDA-SCS, 1972) and is controlled by values of the cumulative precipitation P (mm) during Δt_i and curve number (CN). The value of CN is the main adjustable parameter during model simulation to account for variations of the antecedent moisture condition from event to event and uncertainties in calculating P and CN.

Surface water routing on hillslopes and in stream channels is based on kinematic wave approximations (Borah et al., 2007):

$$\frac{\partial W}{\partial t} + \frac{\partial M}{\partial x} = q \tag{2a}$$

$$M = \alpha W^m \tag{2b}$$

For hillslopes, M is the flow depth (m), W is the water discharge per unit width (m^2/s), and q is the rainfall excess rate (I_e); whereas for stream channels, M is the flow cross section area (m^2), W is the flow rate (m^3/s), q is the lateral inflow rate per unit length (m^2/s), x is the

downslope distance, and t is the time. Kinematic wave coefficient α and exponent m have different values for hillslopes and stream channels, respectively (Borah et al., 2002). Manning's n for overland elements (OMN) and channel segments (CMN) are the two adjustable parameters involved in numerical solutions for Eqs. (2a) and (2b).

Subsurface flow, which ultimately discharges laterally into the contributing channel, is simulated using the well-known kinematic storage equation (Arnold et al., 1998). In DWSM, it is modified for dimensional consistencies and expressed as

$$q_s = K_s sin\beta \frac{2V_w}{L(\theta_s - \theta_d)} \tag{3}$$

where q_s is the subsurface flow per unit overland width (m^2/s), K_s is the lateral saturated hydraulic conductivity (m/s), β is the angle of the impermeable bed in degree, V_w is the drainable volume of water stored in the saturated zone of a unit width of overland (m^3/m), L is the slope length (m), θ_s is the saturated water content (m^3/m^3), and θ_d is the field capacity (m^3/m^3; Borah et al., 2007). Accuracy of predicting this proportion of flow is achieved by adjusting two parameters, effective lateral saturated hydraulic conductivity (COND) and initial uniform moisture content in the soil/porous zone (CONT).

Assuming hillslope surface and channel beds are movable with a detachable soil thickness, DWSM characterizes soil detachment, sediment entrainment and transport, and deposition using the continuity equation based on mass balance for each predetermined grain size class (Borah et al., 2002). Soil detachment rate (E_r, mm/h) is determined using the equation developed by Meyer and Wischmeier (1969), which relates E_r to rainfall intensity, soil cover, and soil properties. During simulation, the value of E_r is calibrated by adjusting the soil detachment coefficient, RDC. Sediment routing through the simulated watershed is based on the mass conservation of the sediment load for any spatially divided lumped unit, which may be mathematically represented as

$$\frac{\partial A_s}{\partial t} + V\frac{\partial A_s}{\partial x} = q_s + g \tag{4}$$

where A_s is the sediment load, expressed as the volume of sediment present in the flow per unit length (m^3/m); V is the average water velocity, expressed as the volumetric rate of lateral sediment inflow per unit length (m/s); q_s is the volumetric rate of lateral sediment inflow per unit length (m^2/s); and g is the volumetric rate of material exchange with the bed per unit length (m^2/s). By definition, $A_s = Q_s/V$ where q_s is volumetric sediment discharge (m^3/s). The value of q_s is calculated using Yalin's equation (Yalin, 1972) and that of Q_s in channels is determined using two total load equations: Yang's equation (Yang, 1977) for coarse sand and Laursen's equation (Laursen, 1958) for fine sand and silts. With this information, the continuity equation may be solved for the potential exchange rate, whose sign and magnitude represent the rate of either deposition or erosion on hillslopes and stream channels. The main adjustable parameter for achieving the best prediction of sediment discharges is flow detachment coefficient (FDC). Previous studies (Gao et al., 2013a, 2015) have shown that predicted sediment discharges are affected much more by the value of FDC than that of RDC.

2.2.2. Spatial arrangement of the study watershed for modeling

In many watershed models, such as SWAT and AGNPS, a target watershed is split spatially into a group of finer-scale areas in terms of the hydrological response unit (HRU), a subarea, either a portion of hillslope or a small subwatershed in which the change of hydrological dynamics is small with respect to its surrounding subareas (Bisantino et al., 2015; Bongartz, 2003; Devito et al., 2005; Dooge, 1968; Flugel, 1995; Kliment et al., 2008; Mishra et al., 2007). In DWSM, however, the study watershed is spatially divided into a number of morphological units, including overland elements interconnected by channel segments. These units may form the first-order and nested subwatersheds, which are conceptually consistent with representative elementary watersheds used in a recently developed network model (Patil et al., 2012). because the sizes of the morphological units are often determined arbitrarily (Mishra et al., 2007; Tripathi et al., 2003), we proposed an objective method that may identify the appropriate number of the units for watershed modeling. First, we generated five sets of overland elements that have different averaged sizes using the ArcHydro model (Maidment, 2002). Second, we calculated percentages of land use/cover (LULC) categorized into each of five classes: crop land (L1), pasture (L2), urban (L3), forest (L4), and others including wetlands and open waters (L5) for each set of delineated overland elements. Because sediment transport is more related to L1, L2, and L3, we created an index (I_s) as the sum of their percentages to quantify the dominant anthropogenic influence on sediment transport in these elements (i.e., $I_s = L1 + L2 + L3$). Third, we calculated mean, maximum, and minimum values of I_s for each set of elements, as well as the mean area (A). Then we examined the trends of these statistical properties against A and identified the most appropriate mean size at which a set of overland elements and the associated channel segments should be delineated.

2.2.3. DWSM input data preparation

Hourly rainfall data during the extreme event from 15 weather stations were downloaded from http://www.srh.noaa.gov/ridge2/RFC_Precip/. These data served as input precipitation values for modeling. Also, they were summed at each station and subsequently used to calculate spatial distribution of total precipitation and the amount of precipitation within each of the delineated overland elements. A single value of parameters representing topographic, vegetation, soil, and sediment properties was assigned to each overland element and channel segment. Values of some parameters such as overland area, slope length, canopy and groundcover densities, and CN were determined directly from the available GIS data. Those of parameters such as the coefficient and exponent of relationships between wetted perimeter and flow area and the size distribution of sediment grains were determined in terms of field measurement performed in our previous studies. Parameters such as OMN, CMN, COND, CONT, and FDC vary among the delineated elements; and their values were estimated using empirical relationships established in terms of previous modeling analysis. Details of calculating values of these parameters may be found in Gao et al. (2015).

Because the flood emerged quickly and overflowed the bank of the cross section where our monitoring station was established, we were unable to collect any data during the flood. Fortunately, we obtained the discharge data from a USGS gauging station located about 1 km upstream of the outlet (Fig. 1). We then converted them into the discharges at the cross section of the outlet and calculated the associated suspended sediment concentrations using the discharge relationship between the two locations and sediment rating curve developed in previous studies (Gao and Josefson, 2012a, 2012b). Using these data, we were able to produce the calculated hydrograph and sedigraph for the modeled extreme event.

2.2.4. Modeling the extreme storm event using DWSM

When modeling a storm event in the study watershed using DWSM, the most sensitive parameters to the predicted hydrograph and sedigraph are CN, OMN, CMN, COND, CONT, and FDC (Gao et al., 2013a). Because the originally determined values of these parameters may not reflect their variability from event to event, we had to adjust them during the simulation to account for the unknown variation and to achieve the best fit to the measured hydrograph and sedigraph. Model predictability was measured by (i) the percent error E_p , which is the ratio of the difference between predicted and measured variables to the measured variable in percentage, for peak water discharge (Q_{peak}) and peak sediment discharge (Q_{speak}); and (ii) E_p and the coefficient of

efficiency, E_c, for event total runoff volume (V), and total sediment yield (TSY_e). The E_c is defined as (Beven, 1993; Licciardello et al., 2007)

$$E_c = \frac{\sum_{i=1}^{n}\left(T_i^p - \overline{\overline{T^m}}\right)^2 - \sum_{i=1}^{n}\left(T_i^p - T_i^m\right)^2}{\sum_{i=1}^{n}\left(T_i^p - \overline{\overline{T^m}}\right)^2} \quad (5)$$

where T is either the water (Q) or sediment (Q_s) discharges, $\overline{\overline{T^m}}$ is the mean of measured T, and T_i^p and T_i^m are the predicted and measured values of T, respectively. Values of E_p describe the event-lumped goodness-of-fit, while those of E_c characterize the degree of synchronization between measured and simulated values over one event. Model prediction is acceptable if E_c is greater than 0.36 (Zema et al., 2010). No widely accepted threshold value of E_p is available for judging model predictability. After achieving the best predictions at the outlet, we used DWSM to estimate event-based variables for all overland elements and stream segments, such as Q_{peak}, V, and TSY_e.

2.3. Analyzing spatial patterns of sediment dynamics during the extreme event

Various spatial patterns of the event sediment dynamics were examined at the smallest spatial scale, which is represented by the group of the delineated overland elements. We showed the spatial distribution of the gross erosion over the extreme event by displaying values of area-specific sediment yield (SSY_e, t/m^2) in all overland elements. To better demonstrate the impact of climatic and environmental factors on sediment transport during the event, we performed nonlinear regression analysis between the total event sediment yield (TSY) and the factors that are commonly related to soil erosion and sediment transport, such as the mean slope (S), land use/cover (LULC), and soil erodibility condition of overland elements (Gao and Puckett, 2012; Kirkby et al., 2002; Mishra et al., 2007), as well as the overland area (A) and mean precipitation (P). Values of S were calculated using DEM data with 10-m resolution as area-weighted slopes in percent. The LULC may be characterized by the percentage of crop and pasture lands (%L), whose values were determined using downloaded National Land Cover Dataset (30-m resolution). The original values of soil erodibility factor (K) were downloaded from the Natural Resources Conservation Service (NRCS) GIS Data Mart and used to calculate the area-weighted value of K for each overland element. Values of P for all elements were calculated in two steps. First, the sum of precipitation for the entire event in each of the 15 stations within the study watershed was used to estimate distributed event precipitation using interpolation analysis in GIS (the Kriging method). Second, the amount of precipitation in each overland element was calculated using zonal analysis after converting the overland shapefile from vector to raster format. Based on established the nonlinear relationship between TSY_e and A, P, S, K, and %L, we examined the overall impact of these variables and their relevant importance on contributing to the sediment load during the extreme event.

The spatial variations of sediment transport during the extreme event were revealed in this study by linking variables representing event sediment loads to those representing hydrological processes of the same event. For overland elements, we examined the relationship between TSY_e and Q_{peak} (m^3/s). At the larger spatial scales, which are represented by the first-order and nested subwatersheds around and along the two main creeks within the study watershed (Fig. 1), we analyzed a variety of statistical relationships between sediment-related variables and hydrological variables. The former include TSY_e, area-specific sediment yield, SSY_e, net erosion/deposition (E/D, t), sediment delivery ratio (SDR), while the latter contain Q_{peak}, A, and event mean runoff depth, h (m), defined as the ratio of event total volume of runoff, V (m^3) to the area of the associated subwatershed, A.

3. Results and analysis

3.1. Morphological units of the study watershed for DWSM and modeling results

Analyzing statistical properties of the index (I_s) showed that while mean values of I_s remained approximately constant, maximum and minimum values of I_s (i.e., I_{sa} and I_{si}) decreased as the mean area of the delineated overland elements (A) increased (Fig. 2). After A = 5.89 km^2, I_{sa} and I_{si} also became roughly unchanged. This value served as a spatial threshold above which the statistical distribution of LULC types among the delineated units is stable. Hence this value represents a reference spatial scale for delineating the study watershed.

Delineation ended up with 42 overland elements and 21 channel segments, which form 21 first-order subwatersheds (Fig. 3). The minimum and maximum sizes of these elements were 1.12 and 15.9 km^2, taking about 0.4% and 5.1% of the study watershed, respectively. Most of the 21 first-order subwatersheds have sizes within 2 to 6% of the study watershed, meaning that they represent the most efficient sizes of subwatersheds for modeling (Jha et al., 2004). Around the main stream, Oneida Creek, there were six first-order subwatersheds, which are associated with channel segments 43, 44, 45, 48, 52, and 54. A combination of subwatersheds 43, 44, and 45 formed the smallest nested subwatershed (denoted as L1). The outlets of the downstream nested subwatersheds were at the end of stream segments 46, 47, 49, 50, 51, 53, and 55 (denoted as L2, L3, L4, L5, L6, L7, and L8; Fig. 3). Along the Sconondoa Creek, the first-order subwatershed was associated with channel segment 61 and the outlets of nested subwatersheds were at the end of segments 56, 57, 58, 59, 60, and 62 (symbolized as R1, R2, R3, R4, R5, and R6; Fig. 3). The two creeks join at the ends of channel segments 55 and 62, and the next larger subwatershed is indeed the entire study watershed.

Based on this spatial arrangement, we performed watershed modeling by adjusting CN, OMN, CMN, COND, CONT, and FDC of DWSM and predicted the hydrograph and sedigraph of the selected extreme event that best fits the calculated ones (Fig. 4a and b). The predicted Q_{peak} and Q_{speak} values were only 3.5% greater than and 4.9% less than the calculated ones, respectively. The small magnitudes of E_p for Q_{peak} and Q_{speak} suggested good model predictions. For V and TSY_e, values of E_p were −24.2% and 38.9%, respectively. Furthermore, their E_c values were 0.73 and 0.52, both of which were greater than the threshold value. Therefore, model predictions were acceptable.

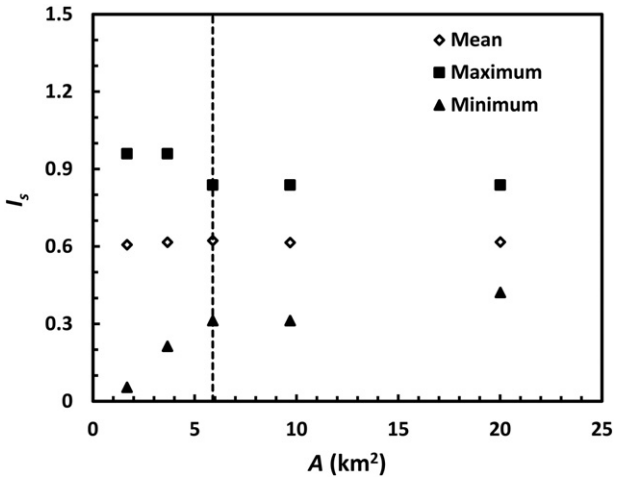

Fig. 2. Plot of the LULC index I_s vs. the mean area of the delineated overland elements, A, for five different spatial arrangements. The dashed line marks the threshold value of A above which the statistical distribution of I_s remains approximately unchanged for the mean, maximum, and minimum areas, respectively.

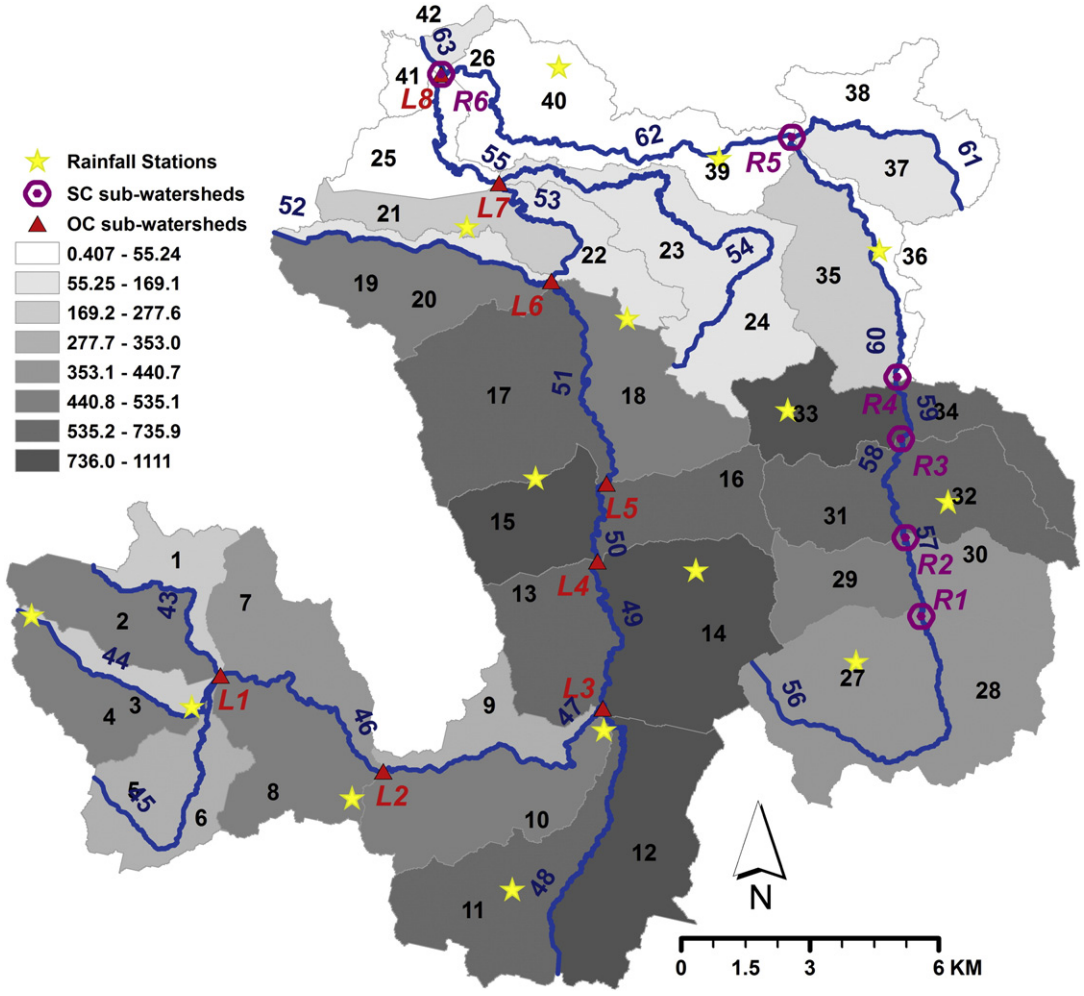

Fig. 3. Spatial arrangement of the study watershed that contains 42 overland elements (1–42) and the associated 21 channel segments (43–63). The red triangles (marked with red labels) represent the outlets of the nested subwatersheds along the Oneida Creek (OC) and the pink circles (marked with pink labels) denote the outlets of the nested subwatersheds along Sconondoa Creek (SC). The yellow stars represent weather stations where rainfall data were obtained and used in modeling. The graduated gray colors represent the predicted area-specific event sediment yields in all delineated overland elements (SSY_e, t/km^2).

3.2. Spatial patterns of event sediment loads among overland elements

Area-specific event sediment yield (SSY_e) varied greatly over all overland elements with the minimum of 0.407 t/km^2 in overland 41 and the maximum of 1110.6 t/km^2 in overland 33 (Fig. 3). Correlation analysis (Table 1) showed that (i) total event sediment yield (TSY_e) was significantly correlated with A, P, and S, and the strength of correlation decreased in this order; (ii) neither K nor $\%L$ was significantly correlated with SSY_e. Based on these results, the subsequent statistical model only included A, S, and P as independent variables:

$$TSY_e = a_1 A^{a2} P^{a3} S^{a4} \quad (6)$$

Nonlinear regression analysis showed that $a1 = 818.2$, $a2 = 1.541$, $a3 = 0.05$, and $a4 = 0.76$ with $R^2 = 0.79$ ($p < 0.0001$). While the model (i.e., Eq. (6)) was statistically significant, the R^2 value was not very high. Comparing the statistically predicted with the model predicted TSY_e values indicated that Eq. (6) described medium and high TSY_e values quite well, but low ones poorly (Fig. 5), suggesting that the not-very-high R^2 value was mainly caused by larger errors in determining relatively low TSY_e values. The values of $a2$, $a3$, and $a4$ further suggested that TSY_e was mainly controlled by the size and then topography of an overland element. Precipitation had a relatively minor impact on TSY_e, though it was the source of surface runoff that caused sediment transport. Consequently, spatial variations of SSY_e cannot be simply explained by either its mean slope or precipitation or both of the associated overland elements. For example, the value of SSY_e in overland 33 was greater than that of overland 12 (870.3 t/km^2), but the former element received less precipitation (59.6 mm) and had gentler slope (0.099) than the latter ($p = 63.3$ mm and $S = 0.134$, respectively).

The statistical model representing the TSY_e-Q_{peak} relationship may be expressed as

$$TSY_e = aQ_{peak}{}^b \quad (7)$$

Nonlinear regression analysis showed that values of a and b for separated data along the two creeks were not drastically different from those for the combined one (Table 2), suggesting that event sediment yields were not spatially segregated. Yet, TSY_e was not well correlated with Q_{peak} (Fig. 6a). Similarly, the statistical model between the area-specific SSY_e and the associated h may be written as

$$SSY_e = ch^d \quad (8)$$

Regression analysis indicated that the SSY_e-h relationship was only statistically significant for the combined data (Table 2, Fig. 6b), further signifying the nonsegregated spatial distribution of sediment yields.

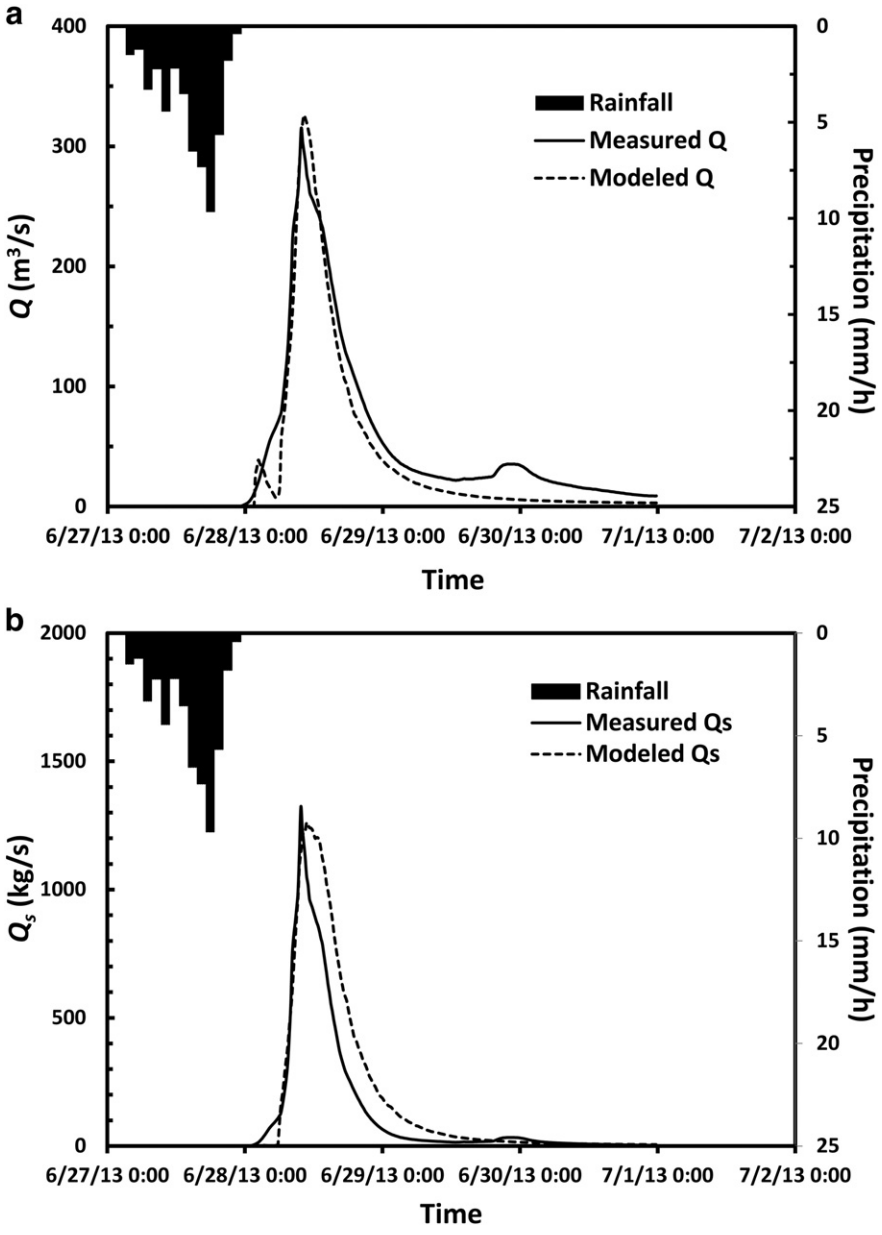

Fig. 4. Comparison between calculated (measured) and predicted hydrographs (a) and sedigraphs (b) for the selected extreme storm event.

Nonetheless, Eqs. (7) and (8) poorly fitted the data (Table 2). Thus, neither event runoff volumes nor peak water discharges were sufficient to capture the complex processes governing sediment transport through these overland elements.

3.3. Spatial patterns of event sediment loads over subwatersheds

Along the two creeks, not only were Q_{peak} values for the first-order and nested subwatersheds correlated with A quite well, but also the two correlations may be characterized by a single linear relationship (Fig. 7). Thus, we only used Q_{peak} as the scale indicator to show spatially variable event sediment loads. From the smallest spatial scale (i.e., the first-order subwatersheds) moving downstream through the nested subwatersheds along the two creeks, TSY_e was generally correlated well with the associated Q_{peak} (the solid curve in Fig. 8). Along OC, the relationship was weakened by two points (i.e., subwatersheds 52 and 54), though it was still statistically significant. Along SC, data points generally followed the same trend except one (i.e., subwatershed 61) and the trend merged into that along OC, suggesting the processes of sediment transport were similar along two creeks during this event. At the

Table 1
Correlations between TSY_e and five environmental parameters for the 42 overland elements (A is the overland area, P is the total precipitation within the overland, S is the mean overland slope, K is the soil erodibility factor of the overland, and $\%L$ is the percentage of crop and pasture lands).

	A		P		S		K		$\%L$	
	R	p-Value	R	p-Value	R	p-Value	R	p-Value	R	p-Value
TSY_e	0.793	<0.0001	0.316	0.041	0.559	0.0001	0.236	0.133	−0.295	0.058

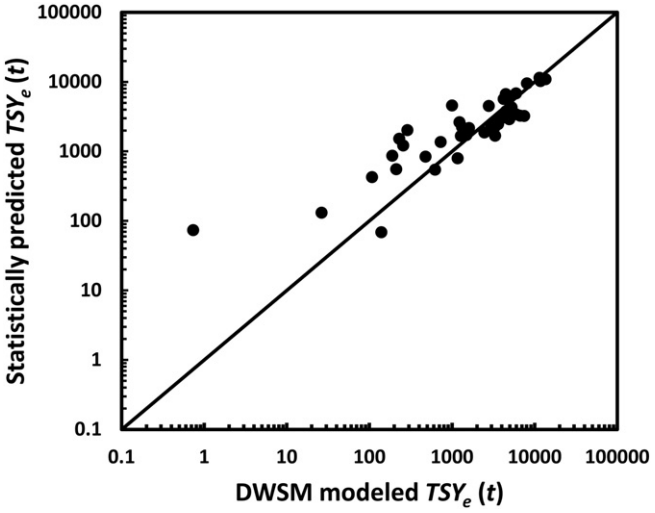

Fig. 5. Comparison of statistically predicted TSY_e values using Eq. (6) for all 42 overland elements with those modeled using DWSM.

largest spatial scale along both creeks (i.e., L8 for OC and R6 for SC), the data points were apparently below the trend, which implies that more deposition occurred within the largest subwatersheds along the two creeks. This might be related to the fact that the two creeks with comparable sizes converge at the outlets of L8 and R6 (Fig. 3). The data point representing values of Q_{peak} and TSY_e at the outlet of the study watershed followed the same trend (Fig. 8). Overall, a single statistical relationship may be used to characterize the spatial changes of TSY_e:

$$TSY_e = 209.1 Q_{peak}{}^{1.0} \qquad R^2 = 0.91, p < 0.0001 \qquad (9)$$

The exponent of Eq. (9) indicated that TSY_e was essentially proportional to Q_{peak}, suggesting that Q_{peak} and TSY_e increased at the same rate from small to large subwatersheds.

Spatially variable sediment dynamics may be further characterized by the spatial variations of sediment transport efficiency, which was quantified by values of SDR (Fig. 9). Although SDR values showed a high degree of variation among the first-order subwatersheds, they were generally high at the relatively small spatial scales along OC. With the increase of the spatial scale, SDR remained approximately constant over a range of areas and then began to drop promptly to the value corresponding to the largest subwatershed. Values of SDR along SC generally followed the trend of those along OC. Apparently, OC transported sediment with a similar efficiency to that of OC during the extreme event.

Table 2
Results of nonlinear regression analyses for Eqs. (7) and (8).

	a	b	R^2	p-Value
OC[a]	1060.1	0.6014	0.214	<0.0001
SC[b]	1216.3	0.3631	0.206	<0.0001
All	1284.7	0.4650	0.189	<0.0001
	c	d	R^2	p-Value
OC	3719.2	0.6399[c]	0.138	<0.0001
SC	754,226	2.3066[c]	0.361	<0.0001
All	11,403.7	1.0	0.194	<0.0001

[a] Oneida Creek.
[b] Sconondoa Creek.
[c] Not statistically significant.

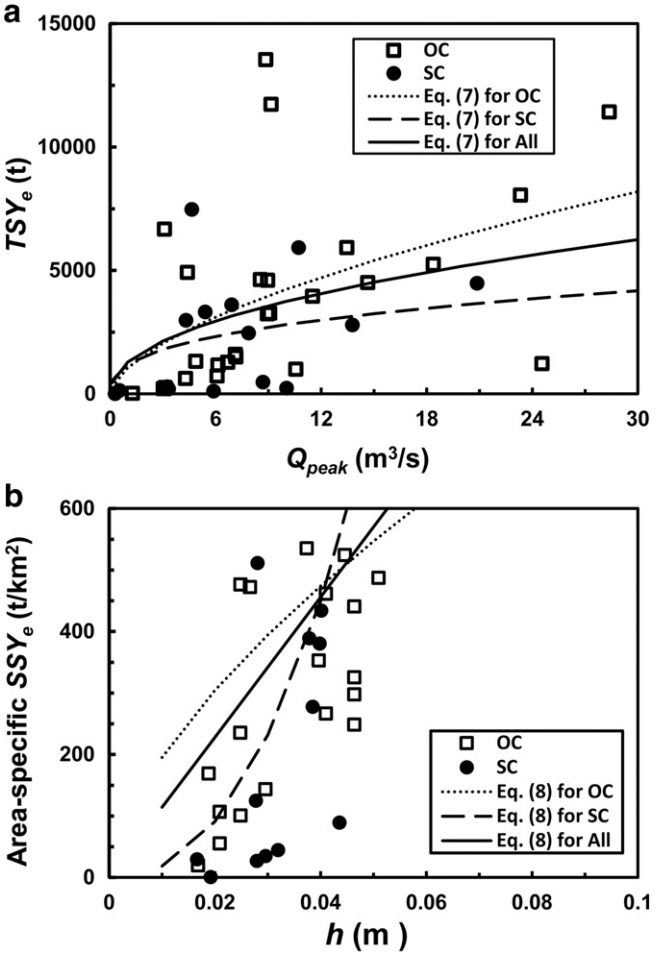

Fig. 6. Statistical relationships for overland elements either around OC or SC, or for all of them. (a) TSY_e vs. Q_{peak}, and (b) area-specific SSY_e vs. h.

4. Discussions

4.1. Uncertainties in model prediction

We have tested the predictability of DWSM in the study watershed by comparing predicted with measured hydrographs and sedigraphs

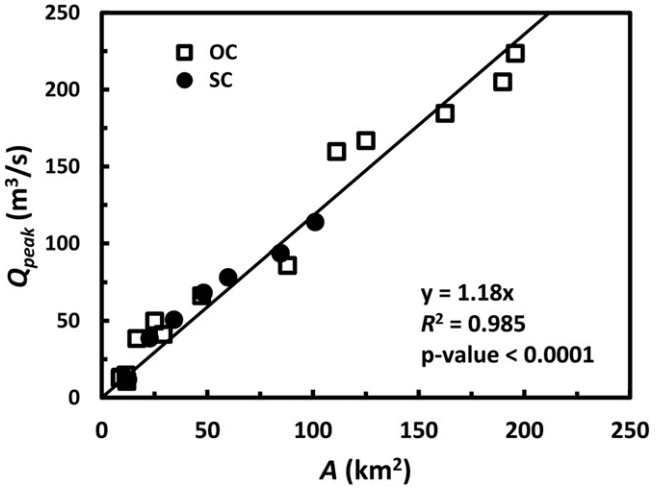

Fig. 7. Plot of peak water discharge (Q_{peak}) of all subwatersheds vs. their areas (A). The solid line represents the statistical relationship between the two.

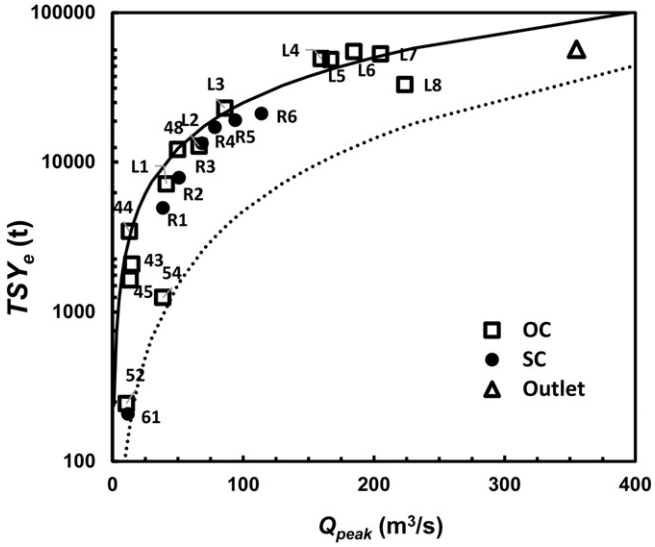

Fig. 8. Plot of TSY_e vs. Q_{peak} for the first-order and nested subwatersheds. The 'outlet' represents the pair of TSY_e and Q_{peak} for the entire study watershed. The solid line represents Eq. (9), and the dashed line denotes the TSY_e-Q_{peak} relationship of many regular events for the entire study watershed (i.e., Fig. 6D in Gao and Josefson, 2012a).

at the outlet of the study watershed for seven storm events with different intensities and magnitudes (Gao et al., 2015). Nonetheless, this test was insufficient to guarantee that the predicted values of Q_{peak}, V, Q_{speak}, and event sediment loads for all overland elements and channel segments were accurate. This is because equifinality (Beven, 1993, 1996), which states that there might be multiple sets of adjustable parameters that can reproduce acceptable transport behaviors of the same watershed, causing the problem typically referred to as predicting the correct result for the wrong reasons (Jetten et al., 2003). In other words, inaccurate hydrological and sediment predictions at some overland elements and channel segments could still lead to reasonably well predictions of hydrographs and sedigraphs at the outlet of the study watershed.

The ideal resolution of avoiding the possible inaccurate predictions at the smaller spatial scales would be measuring Q and sediment concentration (C) at the outlets of all subwatersheds during the simulated event and calculating values of the above-mentioned variables for the event. The predictability of DWSM for all overland elements and channel segments may be then tested by comparing the predicted with measured values. However, it is impossible in practice to accomplish these measurements even during the one that is much less than the selected extreme event.

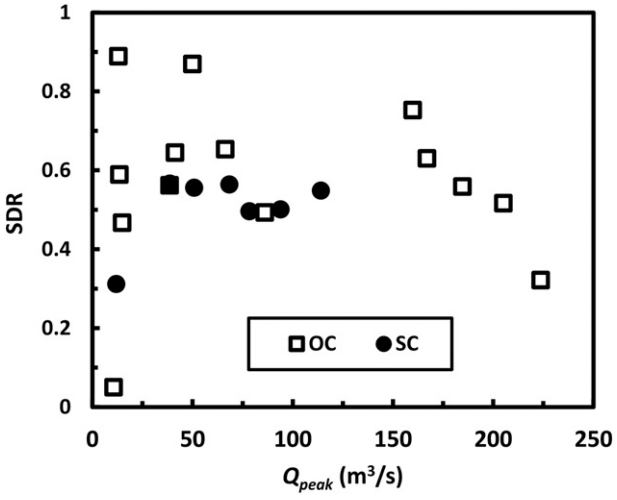

Fig. 9. Plot of sediment delivery ratio (SDR) vs. Q_{peak} for the first-order and nested subwatersheds along OC and SC.

Alternatively, we assessed the model predictability at the finer spatial scales in two indirect ways. First, we know that DWSM performs better during large events than during small events (Borah, 2011). Given that the selected event was an extreme storm event, when DWSM predicted outlet hydrographs and sedigraphs with reasonable accuracies (Fig. 4a and b), we believe the probability of correctly predicting values of the above-mentioned variables for overland elements and channel segments was high. Second, we examined the model predictability at the end of segment 48 (Fig. 3) using previously measured water and sediment data at the site near this location during a small storm event in October 2007 (Gao and Josefson, 2012a). Based on the method described in Section 2.2.3, we calculated hydrograph and sedigraph at the outlet of the study watershed for the same event and produced the best fit by adjusting the previously described most sensitive parameters of DWSM. Then we calculated the predicted V and TSY_e values for the first-order subwatershed associated with channel segment 48. Comparing these two values with the measured values showed that DWSM underestimated V and TSY_e by 21.5% and 32.8%, respectively. The errors may be related to many uncertainties such as the inconsistency between the measured and modeled locations of the selected site, inaccuracy in obtained rainfall data and the single-value parameters assigned to each delineated spatial unit, and errors in the field measurement. Although a more rigorous test of model predictability for event-based sediment dynamics in the delineated overland elements and channel segments is required in the future study, we think the unknown errors involved in the predicted values of the parameters for all delineated small units should not significantly affect the statistical relationships described previously for the selected extreme event.

4.2. Geomorphological significance

Our analysis showed that TSY_e was much better correlated with Q_{peak} at the subwatershed (i.e., larger) scales than at the overland (small) scale (Figs. 6A and 8). This difference might be caused by the different processes controlling sediment dynamics at different spatial scales. Comparing with overland elements, the subwatersheds include not only hillslope hydrological and erosion processes, but also in-channel hydraulic and sediment-transport processes. Thus, the difference in the TSY_e-Q_{peak} relationships suggests that sediment dynamics in subwatersheds was more controlled by in-channel hydraulic processes. This was further evidenced by the much improved correlation between TSY_e and P for the first-order and the nested subwatersheds ($R = 0.90$).

Similar to the Q_{peak}–A relationship (Fig. 7), the Q_{peak}–P relationship was also linear for nested subwatersheds along the two creeks (Fig. 10):

$$Q_{peak} = 0.18P \qquad R^2 = 0.98, p < 0.0001 \qquad (10)$$

These linear relationships were unexpected because hydrological responses to rainfall are generally scale specific and nonlinear (Coulthard et al., 2005; García-Ruiz et al., 2010; Li and Sivapalan, 2011; Marin and Ramirez, 2006; Medici et al., 2008; Wainwright and Bracken, 2011). However, linear relationships were also found in nested watersheds in arid and semiarid regions where intensive but short-duration storms are common (Goodrich et al., 1997). This similarity suggests that the studied extreme storm event generated flash flows at all subwatershed scales, such that flows within the study watershed behaved like those in arid and/or semiarid regions. It highlights the fact that during the extreme storm event in central New York that has a humid, continental climate, the regular flow regime characterized by gentle and long-duration hydrographs with relatively low Q_{peak} values (Gao and Josefson, 2012b; Schneiderman et al., 2007) was changed into a flash flow regime typically occurring in dry lands and, hence, could cause greater damages.

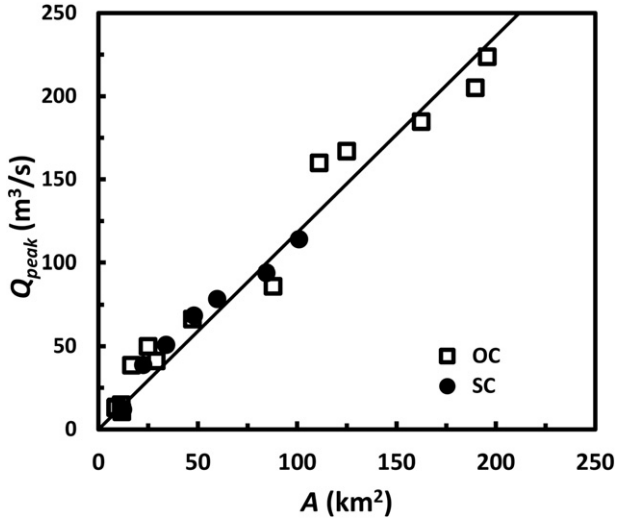

Fig. 10. Plot of Q_{peak} vs. precipitation (P) for the first-order and nested subwatersheds. The solid line represents Eq. (10).

The shift of the flow regime directly improved sediment connectivity, which resulted in two profound changes in sediment dynamics. First, not only was the TSY_e-Q_{peak} relationship much improved compared with that for overland elements (Fig. 8), but also TSY_e increased linearly with Q_{peak} (Eq. (9)). This linear relationship represents the highest degree of sediment connectivity across the entire study watershed at the event temporal scale. In Fig. 8, the dashed curve reflected a nonlinear TSY_e-Q_{peak} relationship (with the exponent >1) for the entire study watershed over many regular storm events (Gao and Josefson, 2012a). Based on this curve, a small Q_{peak} value was a result of a small rainfall event. Yet the same Q_{peak} value could also be generated by the extreme event at a smaller subwatershed but produce a much higher TSY_e than that generated at the outlet of the entire study watershed during the small event, suggesting that the degree of sediment connectivity is low during the small storm event. With the increase of magnitude and intensity of rainfall events, which lead to higher Q_{peak} values, the two TSY_e values become closer, implying the increased degree of sediment connectivity. At the highest available Q_{peak} value, which may be caused by the extreme event, the two SSY_e values approach each other, signifying that the watershed reached the highest degree of sediment connectivity. Theoretically, the two curves should merge at this location. The difference shown in Fig. 8 at this location is mainly caused by the fact that both relationships were developed statistically and hence affected by the uncertainties in the data. A broader implication is that in the American northeast (and other regions) where watersheds have similar climatic and physiographic conditions, sediment loads across multiple spatial scales within a watershed during an extreme storm event reflect the highest degree of sediment connectivity and may be used as a benchmark to quantify the degree of sediment connectivity of a given regular storm event.

Second, the improved sediment connectivity also led to a unique spatial pattern of sediment yields. Because during the extreme event TSY_e was linearly related to Q_{peak} (Eq. (9)) and Q_{peak} was linearly related to A (Fig. 7), TSY_e must be linearly related to A (which was indeed confirmed by the direct regression analysis between TSY_e and A), meaning that area-specific event sediment yield (SSY_e) was constant across all nested subwatersheds during this extreme event. Within a similar range of watershed areas (i.e., from 7 to 311 km^2), annual area-specific SSY_e, which represents sediment yield from all rainfall events within one year, generally increases with watershed size (de Vente et al., 2007). The approximately constant value of area-specific SSY_e implies that sediment transport during this extreme event was probably at capacity, though sediment transport in the study watershed is generally controlled by supply-limited processes (Gao and Puckett, 2012). This may be further supported by the fact that sediment deposition in stream channels increased with the areas of subwatersheds.

The extreme event created a Q_{peak} value of 355 m^3/s (Fig. 4a), more than twice as much as the bankfull discharge (i.e., 150 m^3/s) at the outlet cross section (Gao and Josefson, 2012a). Thus, it is logical to expect that the high flows might have shaped the channels significantly. However, reconnaissance of the river channel in the inundated zone one month after the event showed that there was not much channel morphological change caused by the historical event except some local erosion on the right bank (similar or even larger-scale bank erosion was observed in the past owing to events with much less peak discharges). This limited channel morphological response to the extreme flood reflected the incompetence of the stream flow in shaping channel morphology. Our calculation using previously measured channel reach slope including the studied cross section and the bankfull width showed that the unit stream power of the historical peak discharge was only 32 W m^{-2}. This value is not only much lower than the threshold for causing catastrophic floods, which is 300 W m^{-2} (Lapointe et al., 1998; Magilligan, 1992), but also lower than the low boundary of the channel-forming flow, which is 50 W m^{-2} (Meyer, 2001). Similarly, the calculated area-specific SSY_e was 3.61 t/km^2. It took only 1.4% of the average annual sediment load, which according to our previous analysis is mainly produced by the effective discharge of 65 m^3/s with a recurrence interval of 1.2 years (Gao and Josefson, 2012b). Thus, the historical flood was not large enough to catastrophically alter the channel morphology, nor frequent enough to gradually modify the channel shape.

However, the event overtopped about 700 t of sediment, many of which were deposited in the inundated area of 0.62 km^2 within the city. Cleaning these sediment deposits together with other wastes was one of the major challenges the city officers confronted. These analyses confirmed an earlier finding based on a series of geomorphological analyses for an extreme flood in Vermont — that is, 'short duration, high energy flows can have profound sedimentological effects but have limited erosive, channel widening impacts' (Magilligan et al., 2015, p. 186). It is likely a common geomorphological feature of extreme floods in northeastern watersheds of the USA. The practical implication is that while recurrence interval or bankfull discharge is useful for assessing the potential occurrence of flooding, channel design activities for watershed management should mainly rely on the effective discharge (Biedenharn and Thorne, 1994; Doyle et al., 2005).

5. Conclusions

Using a physically based watershed model, Dynamic Watershed Simulation Model (DWSM), we predicted peak discharge (Q_{peak}), event total runoff volume (V), and event sediment yield for all delineated overland elements and channel segments of a medium-sized watershed in central New York over an extreme storm event. These values were subsequently analyzed to characterize spatial patterns of sediment dynamics over this event within the study watershed. We found that at the overland (i.e., small) scale, total event sediment yield (TSY_e) may be nonlinearly controlled by area, mean slope, and mean precipitation of the delineated overland elements. In addition, TSY_e and area-specific SSY_e were not well correlated with Q_{peak} and event-based mean runoff depth, h, respectively. These findings indicated that sediment dynamics at the overland scale cannot be simply characterized using lumped single values representing area, mean precipitation, and mean slope of overland elements. Across the first-order and nested subwatersheds (i.e., larger scales), however, TSY_e not only was strongly correlated with Q_{peak} but also varied with it linearly. The linearity also existed in the Q_{peak}–A and Q_{peak}–P relationships. The different spatial patterns between the small and large scales were consistent with the fact that in-channel processes were implicit in overland elements, but explicit in subwatersheds, suggesting the increased role of channels

with the increase of the spatial scale. Furthermore, the linear relationships not only revealed the increased degree of sediment connectivity from the small to large spatial scales, but also implied that sediment was transported at capacity during the extreme event. The unique linearity of sediment dynamics signified that spatially variable TSY_e values in overland elements (i.e., the small scale) affected sediment transport in nested subwatersheds (i.e., the larger scales) evenly, such that simply controlling sediment movement from overland elements with higher TSY_e values may not significantly reduce downstream sediment loads if a similar event occurs again.

Acknowledgements

We appreciate the comments and suggestions of the editor-in-chief, Dick Marston and three reviewers, whose insights greatly improved the manuscript.

References

Arnold, J.G., Srinivasan, R., Muttiah, R.S., Williams, J.R., 1998. Large area hydrological modleing and assessment, part I: model development. J. Am. Water Resour. Assoc. 34 (1), 73–89.
Belmont, P., Gran, K.B., Schottler, S.P., Wilcock, P.R., Day, S.S., Jennings, C., Lauer, J.W., Viparelli, E., Willenbring, J.K., Engstrom, D.R., Parker, G., 2011. Large shift in source of fine sediment in the Upper Mississippi River. Environ. Sci. Technol. 45, 8804–8810.
Beven, K.J., 1993. Prophecy, reality and uncertainty in distirbuted hydrological modeling. Adv. Water Resour. 16, 41–51.
Beven, K.J., 1996. Equifinality and uncertainty in geomorphological modeling. In: Rhoads, B.L., Thorn, C.E. (Eds.), The Scientific Nature of Geomorphology. Wiley, Chichester, pp. 289–313.
Biedenharn, D.S., Thorne, C.R., 1994. Magnitude-frequency analysis of sediment transport in the Lower Missippi River. Regul. Rivers Res. Manag. 9, 237–251.
Bisantino, T., Bingner, R., Chouaib, W., Gentile, F., Liuzzi, G.T., 2015. Estimation of runoff, peak discharge and sediment load at the event scale in a medium-size mediterranean watershed using the AnnAGNPS model. Land Degrad. Dev. 26 (4), 340–355.
Bongartz, K., 2003. Applying different spatial distribution and modelling concepts in three nested mesoscale catchments of Germany. Phys. Chem. Earth 28, 1343–1349.
Borah, D.K., 2011. Hydrologic procedures of storm event watershed models: a comprehensive review and comparison. Hydrol. Process. 25, 3472–3489.
Borah, D.K., Xia, R., Bera, M., 2002. DWSM - a dynamic watershed simulation model. In: Singh, V.P., Frevert, D. (Eds.), Mathematical Models of Small Watershed Hydrology and Applications. Water Resources Publications, LLC., Highlands Ranch, Colorado, pp. 113–166.
Borah, D.K., Bera, M., Xia, R., 2004. Storm event flow and sediment simulations in agricultural watersheds using DWSM. Trans. ASAE 47 (5), 1539–1559.
Borah, D.K., Arnold, J.G., Bera, M., Krug, E.C., Liang, X.Z., 2007. Storm event and continuous hydrologic modeling for comprehensive and efficient watershed simulations. J. Hydrol. Eng. 12 (6), 605–616.
Brasington, J., Richards, K., 2007. Reduced-complexity, physically-based geomorphological modelling for catchment and river management. Geomorphology 90 (3–4), 171–177.
Brown, R., Chanson, H., 2012. Suspended sediment properties and suspended sediment flux estimates in an inundated urban environment during a major flood event. Water Resour. Res. 48, W11523 (doi: 11510.11029/12012WR012381).
Cammeraat, E.L.H., 2002. A review of two strongly contrasting geomorphological systems within the context of scale. Earth Surf. Process. Landf. 27, 1201–1222.
Cammeraat, E.L.H., 2004. Scale dependent thresholds in hydrological and erosion response of a semi-arid catchment in southeast Spain. Agric. Ecosyst. Environ. 104, 317–332.
Carpenter, T.M., Georgakakos, K.P., 2006. Intercomparison of lumped versus distributed hydrologic model ensemble simulations on operational forecast scales. J. Hydrol. 329 (1–2), 174–185.
Cavalli, M., Trevisani, S., Comiti, F., Marchi, L., 2013. Geomorphometric assessment of spatial sediment connectivity in small Alpine catchments. Geomorphology 188, 31–41.
Cerdan, O., Le Bissonnais, Y., Govers, G., Lecomte, V., van Oost, K., Couturier, A., King, C., Dubreuil, N., 2004. Scale effect on runoff from experimental plots to catchments in agricultural areas in Normandy. J. Hydrol. 299 (1–2), 4–14.
Chen, L., Zhong, Y.C., Wei, G.Y., Cai, Y.P., Shen, Z.Y., 2014. Development of an integrated modeling approach for identifying multilevel non-point-source priority management areas at the watershed scale. Water Resour. Res. 50 (5), 4095–4109.
CNYRPDB, 2004. A Management Strategy for Oneida Lake and Its Watershed, Central New York Regional Planning and Development Board. Syracuse, New York.
Collins, A.L., Walling, D.E., 2004. Documenting catchment suspended sediment sources: problems, approaches and prospects. Prog. Phys. Geogr. 28 (2), 159–196.
Collins, A.L., Walling, D.E., Webb, L., King, P., 2010. Apportioning catchment scale sediment sources using a modified composite fingerprinting technique incorporating property weightings and prior information. Geoderma 155 (3–4), 249–261.
Coulthard, T.J., Lewin, J., Macklin, M.G., 2005. Modelling differential catchment response to environmental change. Geomorphology 69, 222–241.
Czuba, J.A., Foufoula-Georgiou, E., 2014. A network-based framework for identifying potential synchronizations and amplifications of sediment delivery in river basins. Water Resour. Res. 50 (5), 3826–3851.
de Vente, J., Poesen, J., Bazzoffi, P., Van Rompaey, A., Verstraeten, G., 2006. Predicting catchment sediment yield in Mediterranean environments: the importance of sediment sources and connectivity in Italian drainage basins. Earth Surf. Process. Landf. 31, 1017–1034.
de Vente, J., Poesen, J., Arabkhedri, M., Verstraeten, G., 2007. The sediment delivery problem revisited. Prog. Phys. Geogr. 31 (2), 155–178.
Devito, K., Creed, I., Gan, T., Mendoza, C., Petrone, R., Silins, U., Smerdon, B., 2005. A framework for broad-scale classification of hydrologic response units on the Boreal Plain: is topography the last thing to consider? Hydrol. Process. 19, 1705–1714.
Dooge, J.C., 1968. The hydrologic cycle as a closed system. Bull. Int. Soc. Sci. Hydrol. 13, 58–68.
Doyle, M.W., Boyd, D.S.F., Skidmore, P.B., Dominick, D., 2005. Channel-forming discharge selection in river restoration design. J. Hydraul. Eng. 133 (7), 831–837.
Estrany, J., Garcia, C., Batalla, R.J., 2009. Suspended sediment transport in a small Mediterranean agricultural catchment. Earth Surf. Process. Landf. 34 (7), 929–940.
Evrard, O., Navratil, O., Ayrault, S., Ahmadi, M., Némery, J., Legout, C., Lefèvre, I., Poirel, A., Bonté, P., Esteves, M., 2011. Combining suspended sediment monitoring and fingerprinting to determine the spatial origin of fine sediment in a mountainous river catchment. Earth Surf. Process. Landf. 36, 1072–1089.
Favaro, E.A., Lamoureux, S.F., 2015. Downstream patterns of suspended sediment transport in a High Arctic river influenced by permafrost disturbance and recent climate change. Geomorphology 246, 359–369.
Flugel, W.-A., 1995. Delineating hydrological response units (HRUs) by GIS analysis regional hydrological modeling using PRMS/MMS in the drainage basin of the river Brol, Germany. Hydrol. Process. 9, 423–436.
Forzoni, A., de Jager, G., Storms, J.E.A., 2013. A spatially lumped model to investigate downstream sediment flux propagation within a fluvial catchment. Geomorphology 193, 65–80.
Francipane, A., Ivanov, V.Y., Noto, L.V., Istanbulluoglu, E., Arnone, E., Bras, R.L., 2012. tRIBS-Erosion: A parsimonious physically-based model for studying catchment hydrogeomorphic response. Catena 92, 216–231.
Fryirs, K., 2013. Connectivity in catchment sediment cascades: a fresh look at the sediment delivery problem. Earth Surf. Process. Landf. 38 (1), 30–46.
Fukuyama, T., Onda, Y., Gomi, T., Yamamoto, K., Kondo, N., Miyata, S., Kosugi, K., Mizugaki, S., Tsubonuma, N., 2010. Quantifying the impact of forest management practice on the runoff of the surface-derived suspended sediment using fallout radionuclides. Hydrol. Process. 24, 596–607.
Gao, P., 2008. Understanding watershed suspended sediment transport. Prog. Phys. Geogr. 32, 243–263.
Gao, P., Hartnett, J.J., 2016. Exploring the causes of an extreme flood event in Central New York, USA. Phys. Geogr. 37 (1), 38–55.
Gao, P., Josefson, M., 2012a. Suspended sediment dynamics during hydrological events in a Central New York watershed. Geomorphology 139–140, 425–437.
Gao, P., Josefson, M., 2012b. Temporal variations of suspended sediment transport in Oneida Creek watershed, Central New York. J. Hydrol. 426–427, 17–27.
Gao, P., Puckett, J., 2012. A new approach for linking event-based upland sediment sources to downstream suspended sediment transport. Earth Surf. Process. Landf. 37, 169–179.
Gao, P., Borah, D.K., Josefson, M., 2013a. Evaluation of the storm event model "DWSM" on a medium-sized watershed in Central New York, USA. J. Urban Environ. Eng. 7 (1), 1–7.
Gao, P., Nearing, M.A., Commons, M., 2013b. Suspended sediment transport at the instantaneous and event time scales in semi-arid watersheds of southern Arizona, USA. Water Resour. Res. 49, 1–14. http://dx.doi.org/10.1002/wrcr.20549.
Gao, P., Borah, D., Yi, C., 2015. Storm event flow and sediment simulations in a Central New York watershed: model testing and parameter analyses. Trans. Am. Soc. Agric. Biol. Eng. 85 (5), 1241–1252.
García-Ruiz, J.M., Lana-Renault, N., Beguería, S., Lasanta, T., Regüés, D., Nadal-Romero, E., Serrano-Muela, P., López-Moreno, J.I., Alvera, B., Martí-Bono, C., Alatorre, L.C., 2010. From plot to regional scales: interactions of slope and catchment hydrological and geomorphic processes in the Spanish Pyrenees. Geomorphology 120, 248–257.
Gomi, T., Moore, R.D., Hassan, M.A., 2005. Suspended sediment dynamics in small forest streams of the Pacific Northwest. J. Am. Water Resour. Assoc. 41 (4), 877–898.
Goodrich, D.C., Lane, L.J., Shillito, R.M., Miller, S.N., 1997. Linearity of basin response as a function of scale in a semiarid watershed. Water Resour. Res. 33 (12), 2951–2965.
Gruszowski, K.E., Foster, I.D.L., Lees, J.A., Charlesworth, S.M., 2003. Sediment sources and transport pathways in a rural catchment, Herefordshire, UK. Hydrol. Process. 17, 2665–2681.
Hicks, D.M., 1994. Land-use effects on magnitude-frequency characteristics of storm sediment yields: some New Zealand examples. IAHS Publ. (no. 224), 395–402.
Hicks, D.M., Gomez, B., Trustrum, N.A., 2004. Event suspended sediment characteristics and the generation of hyperpycnal plumes at river mouths: east coast continental margin, North Island, New Zealand. J. Geol. 112, 471–485.
Hooke, J.M., 2003. Coarse sediment connectivity in river channel systems: a conceptual framework and methodology. Geomorphology 56, 79–94.
Houben, P., 2008. Scale linkage and contingency effects of field-scale and hillslope-scale controls of long-term soil erosion: anthropogeomorphic sediment flux in agricultural loess watersheds of Southern Germany. Geomorphology 101, 172–191.
Hunter, N.M., Bates, P.D., Horritt, M.S., Wilson, M.D., 2007. Simple spatially-distributed models for predicting flood inundation: a review. Geomorphology 90, 208–225.
Jetten, V., Govers, G., Hessel, R., 2003. Erosion models: quality of spatial predictions. Hydrol. Process. 17, 887–900.

Jha, M., Gassman, F., Secchi, S., Gu, R., Arnold, J., 2004. Effect of watershed subdivision on SWAT flow, sediment and nutrient predictions. J. Am. Water Resour. Assoc. 40, 811–825.
Jones, K.E., Preston, N.J., 2012. Spatial and temporal patterns of off-slope sediment delivery for small catchments subject to shallow landslides within the Waipaoa catchment, New Zealand. Geomorphology 141–142, 150–159.
Kabir, M.A., Dutta, D., Hironaka, S., 2014. Estimating sediment budget at a river basin scale using a process-based distributed modelling approach. Water Resour. Manag. 28 (12), 4143–4160.
Kirkby, M., Louise, B., Sim, R., 2002. The influence of land use, soils and topography on the delivery of hillslope runoff to channels in SE Spain. Earth Surf. Process. Landf. 27, 1459–1473.
Kliment, Z., Kadlec, J., Langhammer, J., 2008. Evaluation of suspended load changes using AnnAGNPS and SWAT semi-empirical erosion models. Catena 73 (3), 286–299.
Lapointe, M.F., Secretan, Y., Driscoll, S.N., Bergeron, N., Leclerc, M., 1998. Response of the Ha! Ha! River to the flood of July 1996 in the Saguenay region of Quebec: large-scale avulsion in a glaciated valley. Water Resour. Res. 34 (9), 2383–2392.
Laursen, E., 1958. The total sediment load of stream. J. Hydraul. Div. ASCE 54 (HY 1), 1–36.
Leopold, L.B., Wolman, W.G., Miller, J.P., 1964. Fluvial Processes in Geomorphology. W.H. Freeman and Company, San Francisco.
Li, H., Sivapalan, M., 2011. Effect of spatial heterogeneity of runoff generation mechanisms on the scaling behavior of event runoff responses in a natural river basin. Water Resour. Res. 47, W00H08. http://dx.doi.org/10.1029/2010WR009712.
Licciardello, F., Zema, D.A., Zimbone, S.M., Bingner, R.L., 2007. Runoff and soil erosion evaluation by the AnnAGNPS model in a small mediterranean watershed. Trans. ASABE 50 (5), 1585–1593.
Magilligan, F.J., 1992. Thresholds and the spatial variability of flood power during extreme floods. Geomorphology 5, 373–390.
Magilligan, F.J., Buraas, E.M., Renshaw, C.E., 2015. The efficacy of streampower and flow duration on geomorphic responses to catastrophic flooding. Geomorphology 228, 175–188.
Maidment, D.R., 2002. Arc Hydro, GIS for Water Resources. ESRI, Redland.
Makarewicz, J.C., Lewis, T.W., 2003. Nutrients and Suspended Solid Losses From Oneida Lake Tributaries, 2002–2003, Central New York Regional Planning and Development Board. Syracuse, New York.
Marin, S., Ramirez, J.A., 2006. The response of precipitation and surface hydrology to tropical macro-climate forcing in Colombia. Hydrol. Process. 20, 3759–3789.
Medeiros, P.H.A., Guntner, A., Francke, T., Mamede, G.L., de Araujo, J.C., 2010. Modeling spatio-temporal patterns of sediment yield and connectivity in asemi-arid catchment with the WASA-SED model. Hydrol. Sci. J. 55, 636–648.
Medici, C., Butturini, A., Bernal, S., Vzquez, E., Sabater, F., Vélez, J.I., Francés, F., 2008. Modelling the non-linear hydrological behaviour of a small Mediterranean forested catchment. Hydrol. Process. 22, 3814–3828.
Menounos, B., Schiefer, E., Slaymaker, O., 2006. Nested temporal suspended sediment yields, Green Lake Basin, British Columbia, Canada. Geomorphology 79 (1–2), 114–129.
Meyer, G.A., 2001. Recent large-magnitude floods and their impact on valley-floor environments of northeastern Yellowstone. Geomorphology 40, 271–290.
Meyer, L.D., Wischmeier, W.H., 1969. Mathematical simulation of the process of soil erosion by water. Trans. ASAE 12 (6), 754–758 (762).
Mills, C.F., Bathurst, J.C., 2015. Spatial variability of suspended sediment yield in a gravel-bed river across four orders of magnitude of catchment area. Catena 133, 14–24.
Mishra, A., Kar, S., Singh, V.P., 2007. Prioritizing structural management by quantifying the effect of land use and land cover on watershed runoff and sediment yield. Water Resour. Manag. 21, 1899–1913.
Murray, A.B., 2007. Reducing model complexity for explanation and prediction. Geomorphology 90, 178–191.
USDA-SCS, 1972. National engineering handbook, part 630 hydrology, section 4, chapter 10. Natural Resources Conservation Service. U.S. Department of Agriculture.
Navratil, O., Legout, C., Gateuille, D., Esteves, M., Liebault, F., 2010. Assessment of intermediate fine sediment storage in a braided river reach (southern French Prealps). Hydrol. Process. 24, 1318–1332.
Nicholas, A.P., 2010. Reduced-complexity modeling of free bar morphodynamics in alluvial channels. J. Geophys. Res. 115 (*F*4), F04021 (doi: 04010.01029/02010JF001774).
Orwin, J.F., Smart, C.C., 2004. Short-term spatial and temporal patterns of suspended sediment transfer in proglacial channels, Small River Glacier, Canada. Hydrol. Process. 18, 1521–1542.
Owens, P.N., Batalla, R.J., Collins, A.J., Gomez, B., Hicks, D.M., Horowitz, A.J., Kondolf, G.M., Marden, M., Page, M.J., Peacock, D.H., Petticrew, E.L., Salomons, W., Trustrum, N.A., 2005. Fine-grained sediment in river systems: environmental significance and management issues. River Res. Appl. 21, 693–717.
Patil, S., Sivapalan, M., Hassan, M.A., Ye, S., Harman, C.J., Xu, X., 2012. A network model for prediction and diagnosis of sediment dynamics at the watershed scale. J. Geophys. Res. 117, F00A04. http://dx.doi.org/10.1029/2012JF002400.
Pelletier, J.D., 2012. A spatially distributed model for the long-term suspended sediment discharge and delivery ratio of drainage basins. J. Geophys. Res. 117, F02028 (doi: 02010.01029/02011JF002129).
Rustomji, P., Caitcheon, G., Hairsine, P., 2008. Combining a spatial model with geochemical tracers and river station data to construct a catchment sediment budget. Water Resour. Res. 44, W01422. http://dx.doi.org/10.1029/2007WR006112.
Salant, N.L., Hassan, M.A., Alonso, C.V., 2008. Suspended sediment dynamics at high and low storm flows in two small watersheds. Hydrol. Process. 22 (11), 1573–1587.
Schneiderman, E.M., Steenhuis, T.S., Thongs, D.J., Easton, Z.M., Zion, M.S., Neal, A.L., Mendoza, G.F., Walter, M.T., 2007. Incorporating variable source area hydrology into a curve-number-based watershed model. Hydrol. Process. 21, 3420–3430.
Smith, S.M.C., Belmont, P., Wilcock, P.R., 2011. Closing the gap between watershed modeling, sediment budgeting, and stream restoration. In: Simon, A., Bennett, S.J., Castro, J.M. (Eds.), Stream Restoration in Dynamic Fluvial Systems: Scientific Approaches, Analyses, and Tools. AGU, Washington, D.C., pp. 293–317.
Syvitski, J.P., Milliman, J.D., 2007. Geology, geography, and humans battle for dominance over the delivery of fluvial sediment to the coastal ocean. J. Geol. 115, 1–19.
Taguas, E.V., Moral, C., Ayuso, J.L., Perez, R., Gomez, J.A., 2011. Modeling the spatial distribution of water erosion within a Spanish olive orchard microcatchment using the SEDD model. Geomorphology 133 (1–2), 47–56.
Tripathi, M.P., Panda, R.K., Raghuwabshi, N.S., 2003. Indentification and prioritisation of critical subwatersheds for soil conservation management using the SWAT model. Biosyst. Eng. 85, 365–379.
Turnbull, L., Wainwright, J., Brazier, R.E., 2008. A conceptual framework for understanding semi-arid land degradation: ecohydrological interactions across multiple-space and time scales. Ecohydrology 1, 23–34.
Underwood, J.W., Renshaw, C.E., Magilligan, F.J., Dade, W.B., Landis, J.D., 2015. Joint isotopic mass balance: a novel approach to quantifying channel bed to channel margins sediment transfer during storm events. Earth Surf. Process. Landf. 40 (12), 1563–1573. http://dx.doi.org/10.1002/esp.3734.
van Dijk, A.I.J.M., Bruijnzeel, L.A., 2005. Key controls and scale effects on sediment budgets: recent findings in agricultural upland Java, Indonesia. IAHS Publ. (No. 292), 24–31.
Verbist, B., Poesen, J., van Noordwijk, M., Widianto, Suprayogo, D., Agus, F., Deckers, J., 2010. Factors affecting soil loss at plot scale and sediment yield at catchment scale in a tropical volcanic agroforestry landscape. Catena 80 (1), 34–46.
Vericat, D., Batalla, R.J., 2006. Sediment transport in a large impounded river: the lower Ebro, NE Iberian Peninsula. Geomorphology 79, 72–92.
Wainwright, J., Bracken, L.J., 2011. Runoff generation, overland flow and erosion on hillslopes. In: Thomas, D.S.G. (Ed.), Arid Zone Geomorphology: Process, Form and Change in Drylands, third ed. John Wiley & Sons, Ltd, Chichester, UK http://dx.doi.org/10.1002/9780470710777.ch11.
Walling, D.E., 2005. Tracing suspended sediment sources in catchments and river systems. Sci. Total Environ. 344, 159–184.
Walling, D.E., Zhang, Y., 2004. Prediciting slope-channel connectivity – a national-scale approach. IAHS Publ. (no. 288), 107–114.
Warrick, J.A., Bountry, J.A., East, A.E., Magirl, C.S., Randle, T.J., Gelfenbaum, G.R., Ritchie, A.C., Pess, G.R., Leung, V., Duda, J.J., 2015. Large-scale dam removal on the Elwha River, Washington, USA: source-to-sink sediment budget and synthesis. Geomorphology 246, 729–750.
Moreno-de las Heras, M., Nicolau, J.M., Merino-Martín, L., Wilcox, B.P., 2010. Plot-scale effects on runoff and erosion along a slope degradation gradient. Water Resour. Res. 46, W04503. http://dx.doi.org/10.1029/2009WR007875.
Wethered, A.S., Ralph, T.J., Smith, H.G., Fryirs, K.A., Heijnis, H., 2015. Quantifying fluvial (dis)connectivity in an agricultural catchment using a geomorphic approach and sediment source tracing. J. Soils Sediments 15 (10), 2052–2066.
Wilkinson, B.H., McElroy, B.J., 2007. The impact of humans on continental erosion and sedimentation. Geol. Soc. Am. Bull. 119 (1/2), 140–156 (doi: 110.1130/B25899.25891).
Wilkinson, S.N., Prosser, I.P., Rustomji, P., Read, A.M., 2009. Modelling and testing spatially distributed sediment budgets to relate erosion processes to sediment yields. Environ. Model. Softw. 24, 489–501.
Wilson, C.G., Kuhnle, R.A., Bosch, D.D., Steiner, J.L., Starks, P.J., Tomer, M.D., Wilson, G.V., 2008. Quantifying relative contributions from sediment sources in conservation effects assessment project watersheds. J. Soil Water Conserv. 63, 523–532.
Yair, A., Kossovsky, A., 2002. Climate and surface properties: hydrological response of small and semi-arid watersheds. Geomorphology 42, 43–57.
Yalin, M.S., 1972. Mechanics of Sediment Transport. Pergamon Press Ltd., Oxford, UK.
Yang, C.T., 1977. The movement of sediment in rivers. Geophys. Surv. 3, 39–68.
Zema, D.A., Bingner, R.L., Govers, G., Licciardello, F., Denisi, P., Zimbone, S.M., 2010. Evaluation of runoff, peak flow and sediment yield for events simulated by the AnnAGNPS model in a Belgian agricultural watershed. Land Degrad. Dev. 23, 205–215 (doi: 210.1002/ldr.1068).
Zhang, X.F., Zhang, X., Hu, S., Liu, T., Li, G.H., 2013. Runoff and sediment modeling in a peri-urban artificial landscape: case study of Olympic Forest Park in Beijing. J. Hydrol. 485, 126–138.
Zheng, M.G., Cai, Q.G., Cheng, Q.J., 2008. Modelling the runoff-sediment yield relationship using a proportional function in hilly areas of the Loess Plateau, North China. Geomorphology 93, 288–301.
Zheng, M.G., Qin, F., Sun, L.Y., Qi, D.L., Cai, Q.G., 2011. Spatial scale effects on sediment concentration in runoff during flood events for hilly areas of the Loess Plateau, China. Earth Surf. Process. Landf. 36, 1499–1509.
Zheng, M.G., Yang, J.S., Qi, D.L., Sun, L.Y., Cai, Q.G., 2012. Flow-sediment relationship as functions of spatial and temporal scales in hilly areas of the Chinese Loess Plateau. Catena 98, 29–40.
Zhou, Z.X., Li, J., 2015. The correlation analysis on the landscape pattern index and hydrological processes in the Yanhe watershed, China. J. Hydrol. 524, 417–426.